Numerical Computation of Natural Ventilation System at Different Floor for A Multistory Building

M. Z. I. Bangalee, M. Ferdows, Roushanara Begum

Abstract- Dhaka city of Bangladesh has its humble start as a city in 17th century, after the emergence of independent Bangladesh in1971. Natural ventilation system at different floor of a eight storied building is discussed in this study numerically. Mass flow analysis are discussed using velocity vector, and velocity contour. The k − ε turbulence model is used for the computation of nature of the air flow at different height. ANSYS CFX software is used to solve the governing equations. Model is also validated by comparing the result with an experimental result published previously. Bangladesh national building code is applied for modeling the building. Ventilation rate for acceptable indoor air quality is assured by comparing the result with ANSI/ASHRAE Standard 62.1-2004.

Keywords- CFD, k − ε turbulence model, mass flow, natural ventilation, thermal comfort, velocity contour, velocity vector.

1 Introduction

With ever-increasing population, Dhaka as a major metropolis of the country faced tremendous shortage of housing and necessary infrastructures. Most of the city planning initiatives failed to predict the growth of the city in terms of spatial boundary and population (Mahbubun Nabi et. al [2004]). Deficiency in service infrastructures in fringe areas along with other factors forced its inhabitants to live in overcrowded high-rise apartment buildings especially in and around high-class residential areas.

During the past few decades, various symptoms and illnesses have increasingly been attributed to poor indoor air quality. There are some common causes to indoor air pollution include environment around the building, indoor sources of pollution, building design, building materials, building furnishing quality, improper ventilation system, lifestyles, and indoor activities. The air quality investigation of any city or building is a common field of research. Kuo et al. (2008) analyzed the poor indoor air quality of a five star hotel and identified four major problems: low room temperature, insufficient air exchange rate, formaldehyde contamination and the microbial pollution. It was recommended that the hotel rating system in some countries should have not concerned the luxury facilities and services only, the indoor air quality should have been considered to provide healthful and comfortable spaces to the guests as well as to the staffs.

- *M. Z. I. Bangalee is currently an associate professor of Applied Mathematics in Dhaka University, Bangladesh. E-mail: zavid@du.ac.bd*
- *M. Ferdows is currently a of Applied Mathematics in Dhaka University, Bangladesh. E-mail: ferdows@du.ac.bd*
- *Roushanara Begum is currently an assistant professor of Mathematics in American International University Bangladesh, Bangladesh. E-mail: roushan.begum@aiub.edu*

Jantunen (2000) reported that an average person spends 90% of his time indoors. Therefore, the indoor air in residential buildings, offices, schools, or any other populated spaces are of great importance for public health. The parameters that constitute the indoor environment are composition of the air, air flow, temperature, humidity, odor, smokes, dust, chemicals, pollutants, density of population, ventilation system etc. On the international level, International Organization for Standardization (ISO), European committee for Standardization (CEN) and American Society of Heating, Refrigerating and Air Conditioning Engineers (ASHRAE) are reporting and reviewing standards relating to the indoor environment on a regular basis. Nevertheless, most of the standards are related to particular region's weather, pollution, people's adaptation level, performance, economy, lifestyle, clothing etc.

Electricity that makes lives easy and convenient can be termed as the lifeblood of the modern science and technology. In addition, the world's economy highly depends on the electricity production and consumption. The electricity consumption per capita has increased by approximately 122% in the last four decades (World Bank) whereas the global electricity consumption has increased by 31-32% in the first 10 years of twenty first century. The electricity consumption indicator of any country is supposed to be the reflection of the country's economy, technology, and life standard e.g., the United States of America itself consumes more than 20% of the globally produced electricity. It is to be noted that the per capita electricity consumption by the developed countries are almost saturated recently. But it is increasing tremendously in the under-developed or developing countries.

One of the most important methods of saving energy in a building is by carefully designing its facade. A 'double skin facade' is optimally one of the best options in managing the interaction between the outdoors and the internal spaces. It also provides some architectural flexibility to the design (W.

Oesterle et al. [2001]). Ding et al. [2005] defined it as "Double-skin facade is composed of an external facade, an inter-mediate space and an inner facade. The outer facade layer (glazing) provides protection against the weather and improved acoustic insulation against external noise. An adjustable sunshade device, such as blinds, is usually installed in the intermediate space to protect the internal rooms from high cooling loads caused by insulation".

To simulate the urban wind flowing across the neighborhood, CFD as an effective tool (An-Shik Yang et al. [2013]). The micro-climatic conditions of the city can also be characterized before the development and settlement of design strategies. The review of scientific and technical literature is conducted by Manfred J. Zapka et al. [2014] to identify previous published research in areas that pertain to predicting airflow inside of buildings with the help of Computational Fluid Dynamics (CFD) investigation.

CFD is an appropriate and reliable method of ventilation performance prediction for multi-storey buildings, where it able to predict ventilation rate and capture changes on indoor airflow pattern (M. F. Mohamed et al. [2010]). It is also concluded that for a tall building with cross ventilation strategy, CFD coupled outdoor and indoor airflows simulation provides acceptable predictions of ventilation rate, except for units located at the bottom of the building.

The natural ventilation system presents a challenge and thus appropriate methods are required, which can help in optimal design of natural ventilation by providing qualitative and quantitative information on the interactions between the microclimate conditions and the building. The CFD models are most popular for predicting ventilation performance in the research community. The use of CFD with other building simulation tools to enhance its ability and to reduce computing costs seems attractive. 70% of the ventilation performance studies which were published in the past years are based on CFD models (Qingyan Chen 2008).

2 MODEL GEOMETRY

An eight-storied building is taken enclosing 80% area (5760 ft²) of total lot area (7200 ft²)to comply with the building code for Dhaka city. 80% maximum allowable building footprint (MABF) is chosen because it is the most common building type in Bangladesh [Saiful Islam, 2012 & 2013], though 70% MABF is the best option to be chosen. Each floor has four units (Fig. 1a) of equal area (38 ft × 35 ft or 11.585 m × 10.67 m). The height of the building is 26.4 m. The area for staircase is 160 ft² (14.872 m²).

Each of the units has three living rooms, two bathrooms and a kitchen room (Fig. 1a), which is the most common interior design in Bangladesh. To choose the dimension of each room, door or window position, ceiling height of each floor, Bangladesh National Building Code-2012 [2012] is followed. 0.5 m thickness is kept for the outer walls and the ceilings and 0.3 m thickness is kept for the inner partitions between any two rooms. Height of each floor is 2.8 m (without ceiling thickness). The dimension of each of the living rooms is 4.698 m ×4.698 m (15 ft ×15 ft). The dimension of the kitchen room is 3.659 m × 3.049 m (12 ft × 10 ft) and each of the bath rooms is 3.049 m × 2.439 m (10 ft × 8ft). The remaining floor area may be used as the dining space.

The dimension of the exit door is 3.5 ft × 7 ft (width × height). The dimension of each of the doors of living rooms is kept same as the exit door. The dimension of the kitchen and bath room doors is kept as 3 ft × 7 ft (width × height). In total six windows are kept in each unit (one at living room-1, two at living room-2 and one at each of the bath and kitchen room). Each of the windows of living rooms is 6ft × 4.5 ft (width × height) at the height of 0.762 m from the floor. The window of the kitchen room is 4.5 ft × 3.5 ft (width × height) at the height of 1.22 m from the floor and the window of the bath room is 3.5 ft × 1.64 ft (width × height) at the height of 1.995 m from the floor. Two windows are also kept at the staircase area (one at the south wall and other at the north) each of 4.5 ft ×3 ft (width × height) at the height of 1.22 m from the floor.

Extended computational domain is assumed around the building to observe the flow phenomena outside the buiding as shows in Fig. 1b.

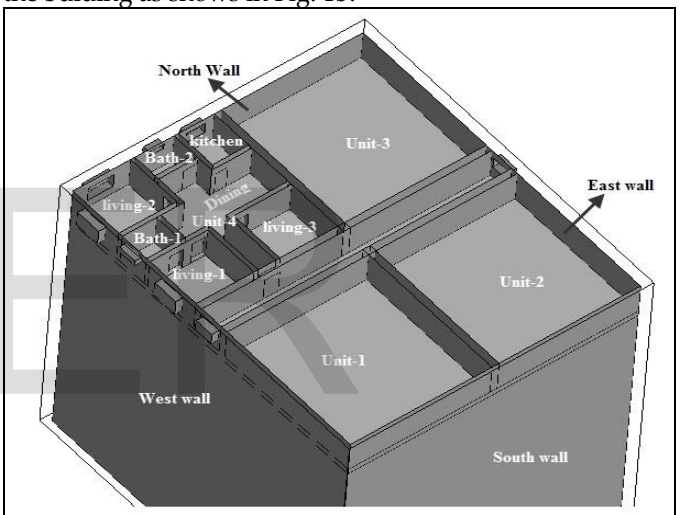

Fig.1a: Unit distribution in top floor, room partitions, doors and windows in a unit.

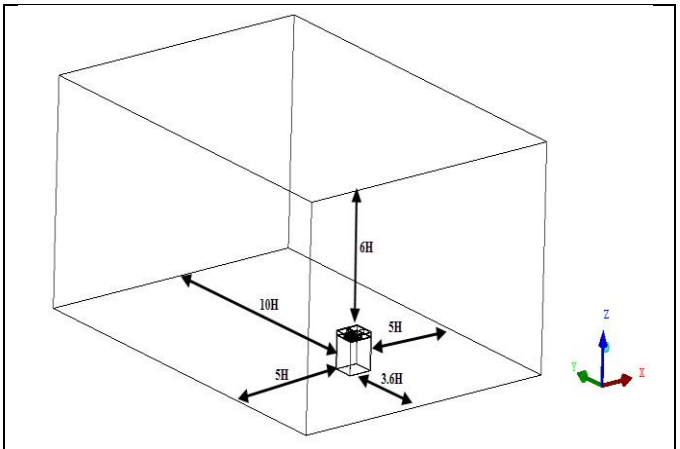

Fig. 1b: Surrounding distance from all the sides of the building.

3 Grid analysis

Grid analysis is performed by considering all the windows and doors as closed except interiors of unit -1. So,

fluid only enters through the windows of unit -1. Unstructured mesh is generated for numerical simulation. Fig. 2a shows the volume mesh through the building and extended computational domain. Fig. 2b shows the surface mesh on the extended computational domain surface and on the surface of unit-1. Denser mesh is confirmed close to the windows and the boundary walls.

Among the five different grids, Grid-4 with 2544904 tetrahedron elements is chosen for further simulation. Maximum element of Global mesh size of Grid-4 is 7500 with scale factor 1 with part mesh. Maximum element size at the inner layer of the building boundary and at the window frames is set as 200. Maximum element size is 450, at the outer layer of the building boundary and is 4000, at the extended computational domain boundary.

Difference in mass flow average velocity through one of the windows opening with Grid-3 and Grid-4 is presented in Tabel-1. It is observed from the table that difference with Grid-4 in mass flow average velocity has negligible effects on grid. If we increase the total number of elements, change in average velocity is negligible (2.75%).

Table 1
Difference in Mass Flow Average Velocity in an Opening Position

Grid (No. of elements)	Grid-1 (454911)	Grid-2 (995884)	Grid-3 (1653880)	Grid-4 (2544904)	Grid-5 (3539246)
Converged residual	10^{-3}	10^{-4}	10^{-5}	10^{-4}	10^{-3}
Mass flow average velocity [m/s]	0.66866	0.672356	0.76309	0.802504	0.824591
Difference with Grid-4	-16.68%	-16.22%	-4.9%	-	2.75%
Difference with Grid-3	-12.37%	-11.89%	-	5.17%	8.06%

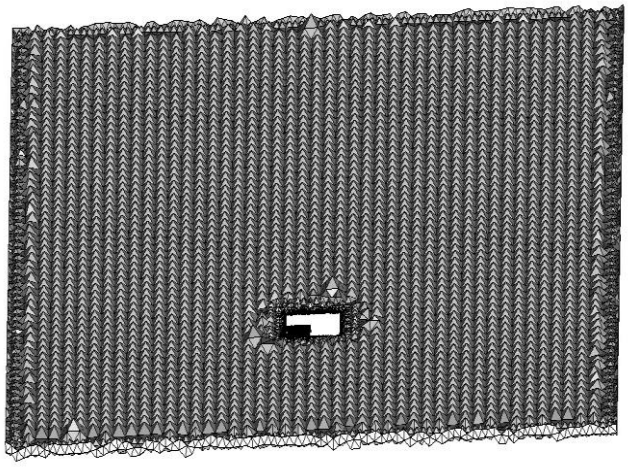

Fig. 2a: Volume mesh on a cut plane through the building and extended computational domain.

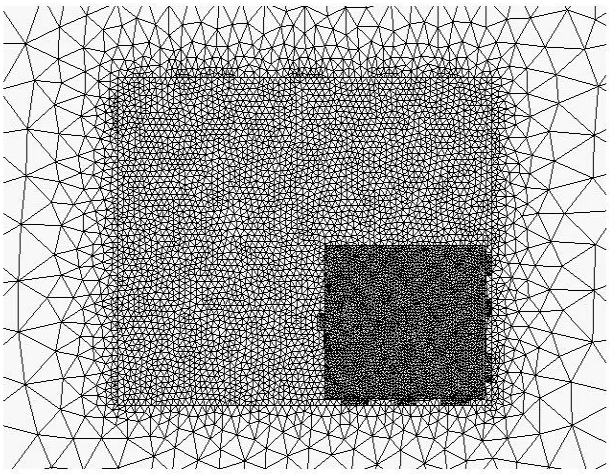

Fig. 2b: Surface mesh on the building and denser mesh close to the building boundary.

4 Methodology

Nomenclature

u, v, w	X, Y, Z-components of velocity respectively [ms^{-1}]
x, y, z	Cartesian coordinates [m]
β	Thermal expansion coefficient [K^{-1}]
μ	Dynamic viscosity [Kg m^{-1}s^{-1}]
μ_T	Turbulence viscosity [Kg m^{-1}s^{-1}]
ν	Kinematic viscosity [m^{2}s^{-1}]
ρ	Density of the fluid [Kg m^3]
σ_T	Thermal diffusivity [m^{2}s^{-1}]
C_n	Specific heat capacity [J Kg^{-1}K^{-1}]
Gr	Grashof number [-]
L	Length [m]
W	Width [m]
H	Height [m]
P	Pressure [Kg m^{-1}s^{-2}]
k	Turbulent kinetic energy [m^{2}s^{-1}]
g	Gravitational acceleration [ms^{-2}]
ε	Dissipation rate
Pr	Prandtl number [-]
Ra	Rayleigh number [-]
Nu	Nusselt number [-]
T*	(T-Tc)/ ΔT

4.1 Governing equations and boundary conditions

CFD is based on the resolution of the governing equations which describe the flow field in the computational domain, namely the continuity equation for mass transfer, the Navier-Stokes equation for momentum transfer and the thermal energy equation for heat transfer. These equations for this problem can be written as follows:

Continuity equation:

$$\frac{\partial}{\partial x_j}(u_j) = 0; \quad j = 1, 2, 3; \qquad (3.1)$$

Momentum equation:

$$\rho u_j \frac{\partial}{\partial x_j}(u_i) = -\frac{\partial p}{\partial x_i} + \frac{\partial}{\partial x_j}[(\mu + \mu_T)\frac{\partial u_i}{\partial x_j}] + \rho_{ref} g_i \beta (T - T_{ref});$$

$$i = 1,2,3;\ j = 1,2,3; \quad (3.2)$$

Energy equation:

$$u_j \frac{\partial}{\partial x_j}(T) = \frac{\partial}{\partial x_j}[(\frac{\nu}{\Pr} + \frac{\nu_T}{\sigma_T})\frac{\partial T}{\partial x_j}];\ j = 1,2,3; \quad (3.3)$$

According to the $k-\varepsilon$ model, μ_T can be expressed as follows:

$$\mu_T = C_\mu \rho \frac{k^2}{\varepsilon} \quad (3.4)$$

k and ε can be obtained from the following equations:

$$\frac{\partial}{\partial x_j}(\rho u_j k) = \frac{\partial}{\partial x_j}[(\mu + \frac{\mu_T}{\sigma_k})\frac{\partial k}{\partial x_j}] + P_k - \rho\varepsilon;$$

$$j = 1,2,3; \quad (3.5)$$

$$\frac{\partial}{\partial x_j}(\rho u_j \varepsilon) = \frac{\partial}{\partial x_j}[(\mu + \frac{\mu_T}{\sigma_\varepsilon})\frac{\partial \varepsilon}{\partial x}] + C_1 \frac{\varepsilon}{k} P_k - C_2 \rho \frac{\varepsilon^2}{k};$$

$$j = 1,2,3; \quad (3.6)$$

Here P_k is the production rate of turbulent kinetic energy which depends on the turbulent viscosity and velocity distribution. The values of all the empirical constants used in previous equations are presented in Table 2.

Table 2
Empirical Constants Used in $k-\varepsilon$ Model

C_μ	0.09
C_1	1.44
C_2	1.92
σ_k	1.0
σ_ε	1.3

4.2 Boundary conditions

The following boundary conditions and locations are used at 25^0 C isothermal temperature:

i. Opening at zero relative pressure: North wall of the computational domain
ii. No-slip wall with 0.28mm roughness: Ground of the computational domain
iii. Symmetry wall: Top, east and west walls of the computational domain
iv. No-slip wall with 0 mm roughness: Building outer layers
v. No-slip and smooth wall: Building inner layers, door and window frames
vi. Inlet boundary conditions: Following inlet boundary conditions are used at the south wall of computational domain:

Normal speed, $U(z) = \frac{u^*}{k}\ln(\frac{z+z_0}{z_0})$

$$u^* = \frac{0.42 U_{ref}}{\ln((H+z_0)/z_0)}$$

$$I(z) = \frac{1}{\ln(z/z_0)}$$

$$k(z) = (I(z) * U(z))^2$$

$$\varepsilon(z) = \frac{u^{*3}}{0.42(z+z_0)}$$

Where U_{ref} = 1.28 m/s, which is the average wind speed at Dhaka during the month of October (Bangladesh metereological department), when this simulation was being done.
Z_0 = 0.000025m,
H=26.4 m, which is the total height of the building.
Velocity increases with the increase of height.

5 Model Validation

G. Evola and popov [2006] has discussed numerical results for single sided ventilation system and Jiang et al. [2003] has discussed experimental results for single sided and cross ventilation system. Cross ventilation is one of the most common ventilation patterns in wind driven natural ventilation system. In cross ventilation system, two or more openings are present in opposite sides of the building. Karava et al. [2011] reported an experimental result for cross ventilation opening in two opposite walls at different height. Comparison with the result of Karava et al. [2011] is presented here to validate the numerical method used for further simulation.

5.1 Comparison with the results reported by Karava et al. [2011]

The experimental study of wind driven cross ventilation flow based on particle image velocimetry (PIV) method in a boundary layer wind tunnel is reported by Karava et al. [2011]. A reduced scale model of dimensions 100 mm × 100 mm × 80 mm (width × length × height) with 2mm thick walls had chosen for experimental work corresponding to full-scale dimensions 20 m × 20 m × 16 m (width × length × height). Nine different opening positions were considered in two opposite walls. Three different sizes (5%, 10% and 20% wall porosity) of each opening were evaluated. For varying wall porosity, the openings had a fixed height of 18 mm and a variable width.

In this study, case E1 (both openings are at the center of two opposite walls) is simulated and compared with experimental results for 5% and 10% wall porosity. Fig. 4 shows the schematic view of the cross-ventilation model with 10% wall porosity. Dimensions of the computational domain is chosen at 5H away from both the lateral sides, 3H away from the front wall, 15.25H far from rear wall and 5H far from the roof of the building. Here H = 80mm is the reference height. The velocity profile on the line through mid-points of the inlet and outlet opening and velocity vectors on the vertical plane at mid width are observed for comparison.

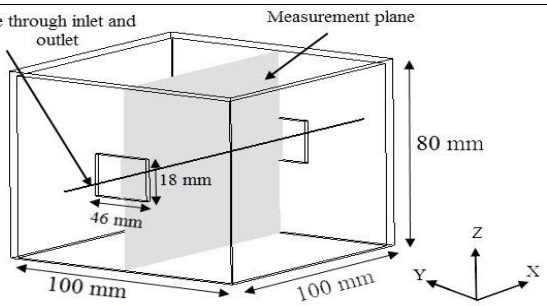

Fig. 4: Schematic view of the wind driven cross ventilation model with measurment plane and line (10% wall porosity).

A non-uniform structured mesh is also generated here for both the building and computational domain. In case of 10% wall porosity, $61\times118\times97$ non-uniform mesh and about 0.69 million elements in the building and $140\times125\times76$ non-uniform mesh and about 1.23 million elements in the computational domain with stretching factor 1.2 and minimum spacing 0.5 mm is used for grid generation. Denser mesh is used around the openings and building surfaces. Similar grid distribution is used in case of 5% wall porosity. Fig. 5(a) and 5(b) show the grid distribution in the building and the computational domain.

The following inlet boundary conditions proposed by Karava et al. [2011], Ramponi and Blocken [2012] are applied:

$$u^* = \frac{0.42U_{ref}}{\ln((H+z_0)/z_0)}$$

$$U(z) = \frac{u^*}{k}\ln(\frac{z+z_0}{z_0})$$

$$I(z) = \frac{1}{\ln(z/z_0)}$$

$$k(z) = (I(z)*U(z))^2$$

$$\varepsilon(z) = \frac{u^{*3}}{0.42(z+z_0)}$$

Where U_{ref} = 6.97 ms^{-1}, z_0=0.025 mm.

The sand grain roughness height of 0.28 mm is used at the ground surface and zero roughness height is used at the building surfaces. Symmetry condition is used at the lateral and top surrounding boundaries. Zero pressure is used at the outlet opening.

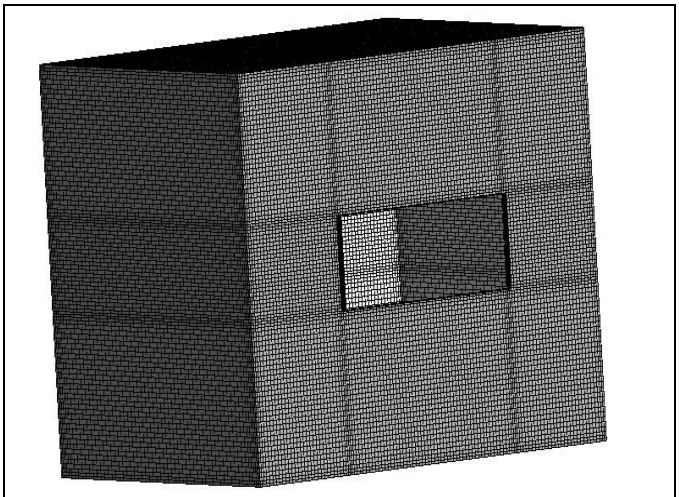

Fig.5 (a): Grid distribution in the building

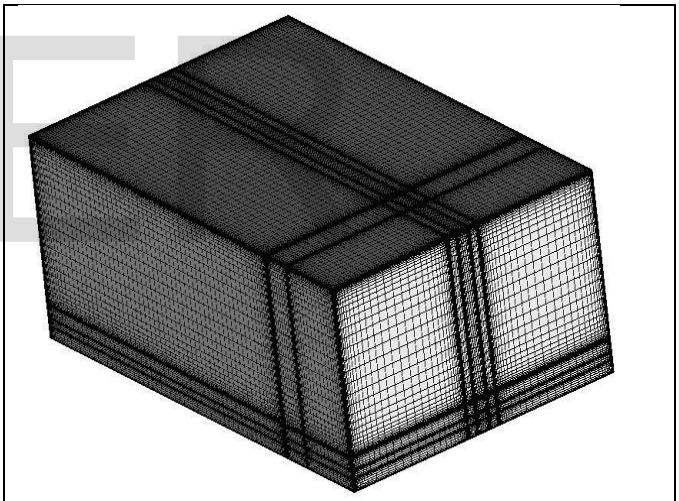

Fig.5 (b): Grid distribution in the extended computational domain.

The simulations were performed for different turbulence model such as $RNG\,k-\varepsilon$ model, Shear Stress Transport ($SST\,k-\omega$) model, $k-\varepsilon$ and $k-\omega$ model. Fig. 6(a) and Fig. 6(b) show the velocity profile along a line through the center of the openings. The comparison is presented between the results using these models and the experimental result for 10% and 5% wall porosity respectively. Good agreement is found with the experimental results. $RNG\,k-\varepsilon$ and $SST\,k-\omega$ give better results than other two models. It can also be seen that, among all these models, $RNG\,k-\varepsilon$ model shows best agreement with the experimental result. Fig. 6c shows the velocity vector on a vertical plane at the mid width of the building using $RNG\,k-\varepsilon$ model. Good agreement is also observed here. Table 3 shows the required time for 100 iterations in each turbulence model. It is also clear from the

table that $RNG-k-\varepsilon$ model needs less time than other models.

Though the $RNG\,k-\varepsilon$ turbulence model may be suitable to predict the flow phenomena for cross ventilation system accurately, in this study, $k-\varepsilon$ turbulence model is used because of convergence problem with $RNG\,k-\varepsilon$ turbulence model.

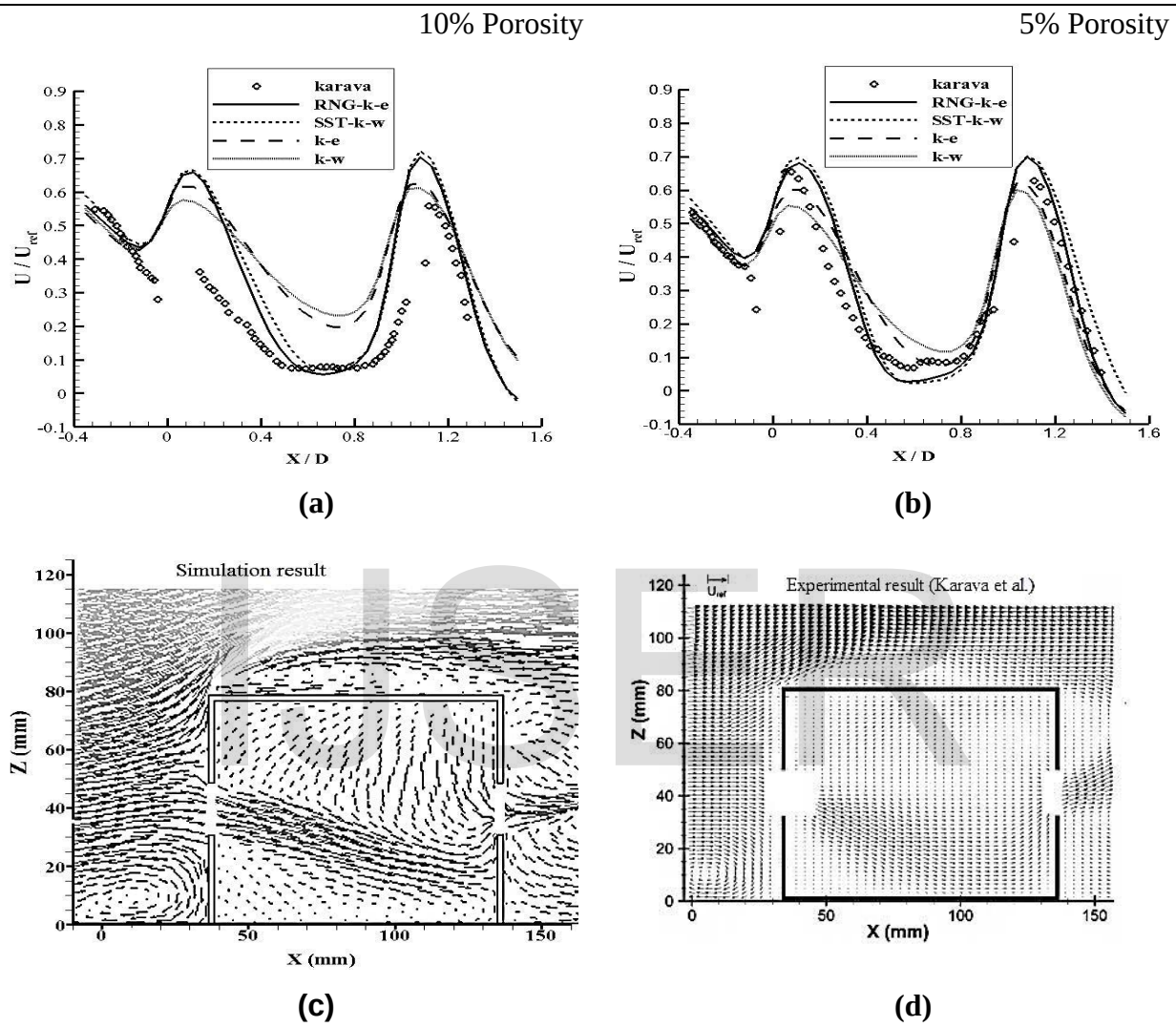

Fig. 6: Comparisons of velocity distributions between experimental and simulation results

6 Result Analysis

6.1 Flow analysis in Unit-1 located in eighth floor

Flow analysis through the windows and inside one of the units of eighth floor (height = 23.1 m to 25.9 m) keeping Unit-1 open only is discussed here briefly. In this case, only the windows of unit-1 of eighth floor are kept open and all other windows and doors are assumed to be closed so that air is entering to this unit only. Also the inner room partitions are not considered here. Unit-1 is at the south-west corner of the buiding (Fig. 1). For the convenience of the discussion, planes through the six windows in each unit are numbered as plane-1, plane-2 etc. as shown in Fig. 7.

In this study, south wall is cosidered to be the front wall of the building. Boundary conditions at the inlet, outlet and other walls are used as the experimental work conducted by Karava et al. [2011] which are discussed in method verification section. South wall is assumed as inlet and north wall as outlet. The reference velocity is assumed to be 1.28 m/s which is the average wind speed at Dhaka during the month of October (Bangladesh metereological department), when this simulation was being done.

Fig. 8(a) and 8(b) shows the velocity distribution of the airflow inside the unit-1 through the mid width and length respectively at the mid-height of this unit. From both of this figure it is observed that velocity is higher closed to

the boundary and lower around the mid-position of this unit.

It is observed from this figure that windows at the south wall are behaving as inlet and windows at west wall are behaving as outlet such that the air is entering through these inlets and exiting through these outlets. Velocity vectors and velocity contours at the planes through these windows are also shown in Fig. 9 and Fig. 10 respectively.

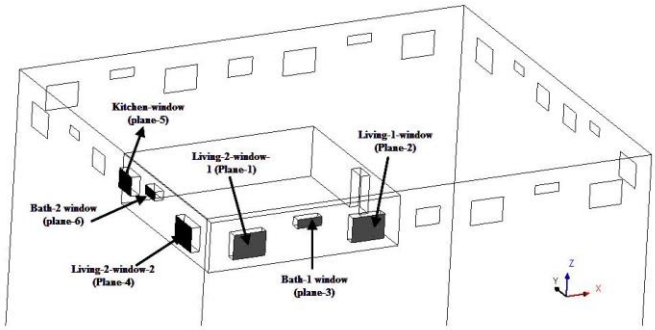

Fig. 7: Unit-1 with all windows and corresponding plane no.

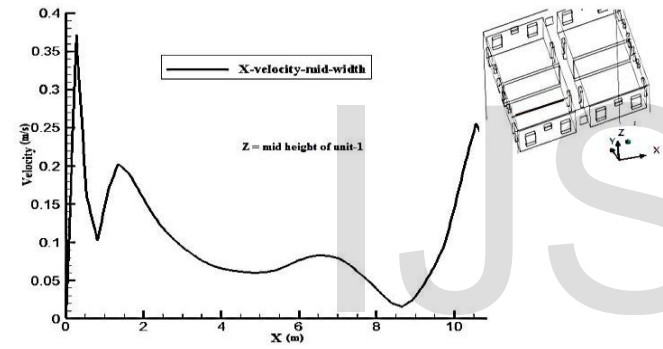

Fig. 8(a):Velocity profile at mid-height and through the mid width of unit-1.

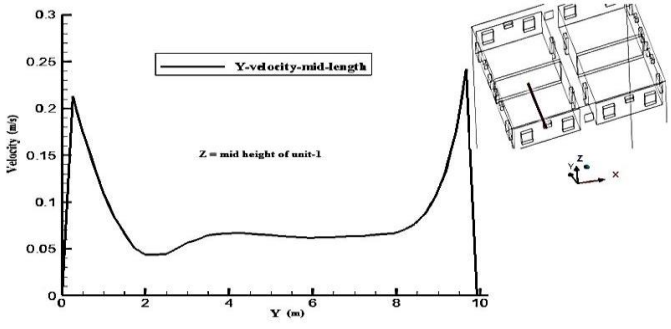

Fig. 8(b):Velocity profile at mid-height and through the mid length of unit-1.

It is clear that the velocity is close to zero m/s near the window frames as expected and velocity is higher around the mid-position of the windows.

Fig. 11 shows the velocity profiles at the windows. These velocity profiles are drawn at different height (top, mid and bottom positions) of each window. It is observed from these figures also that velocity is higher at the mid-position of each window. And it is almost zero m/s both at the top and bottom sides (close to the frames) of the window. So, it may be concluded that air is entering and exiting to the buiding with higher velocity through the mid position of the window. It is occurred beacause air gets obstacle at the frames of the windows while entering to or exiting from the building.

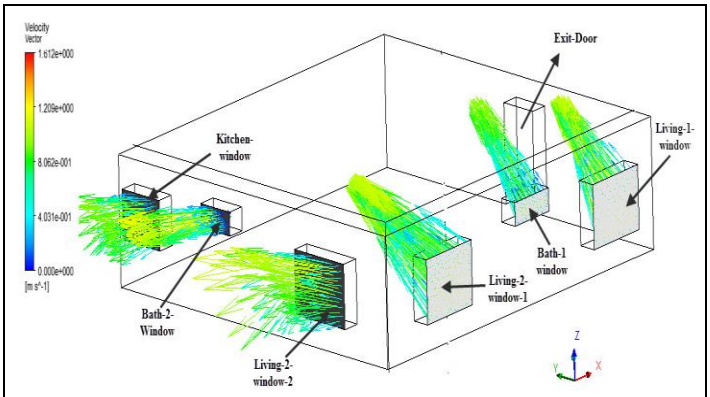

Fig. 9: Velocity vectors through all the windows of unit-1.

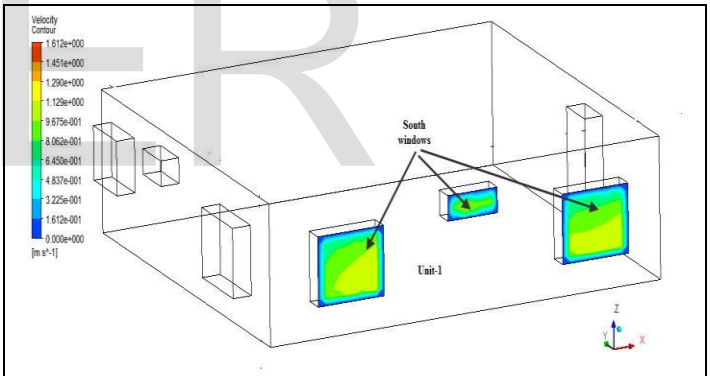

Fig. 10(a): Velocity contours through the south wall windows of unit-1.

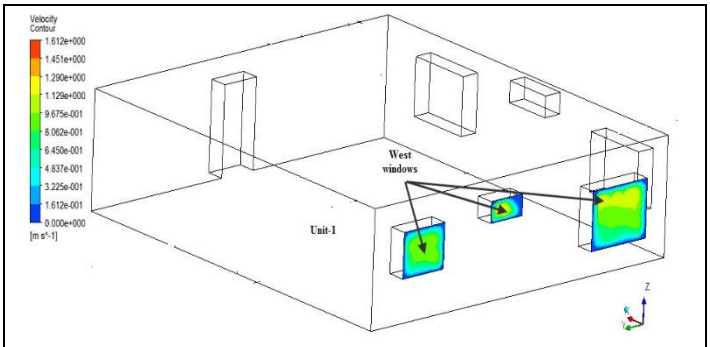

Fig. 10(b): Velocity contours through the west wall windows of unit-1.

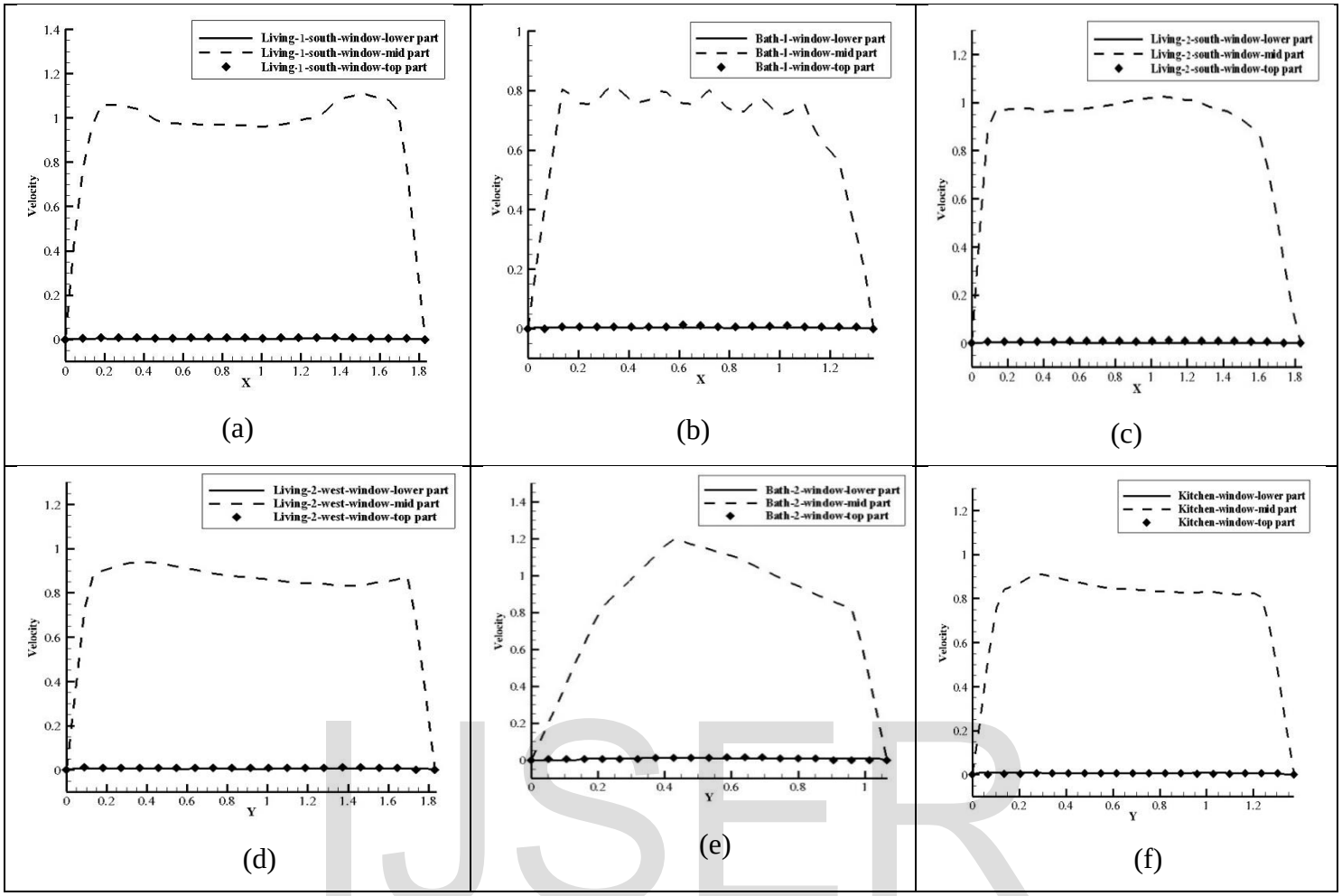

Fig. 11: Velocity profiles at different positions of the window

6.2 Comparison and flow analysis in Unit-1 and Unit-4 of fifth floor

Flow analysis in eighth floor, fifth floor and second floor is observed in this study. Flow analysis in fifth floor (height = 13.2 m to 15 m) with and without the room partitions in unit-1 and unit-4 are represented in this section. Average velocity and mass flow through different windows of unit-1 and unit-4 with room partitions are shown in Table-3. It is observed that mass flow rate in fifth floor is lower than eighth floor. It is because the velocity of the fluid (air) decreases with the decrease of height. Velocity vectors (Fig. 12 & Fig 13) shows the same airflow direction as eighth floor.

Fig. 14 and Fig.15 show the velocity contours on different planes through different windows of unit-1 and unit-4 with all the room partitions in fifth floor. It is observed that velocity is lower in this floor than eight floor. Fig. 16 and Fig. 17 show the velocity vectors through different windows of unit-1 and unit-4 without room partitions. It is shown that there is negligible effect on velocity vectors between the cases with and without room partitions.

Some visible changes are observed on plane-1 (Living-1 window) and plane-3 (Bath-1 window). It is because of the position of the doors in these rooms (Living-1 and Bath-1). Doors and windows are on two adjacent walls of these rooms. Other windows are on two opposite walls of each room. Air can pass the through the doors directly while entering or leaving the rooms.

Table 3
Average mass flow through different windows of unit-1 and unit-4 with room partitions

Position	Area (m^2)	Density (Kg/m^3)	Average velocity (unit-1) (m/s)	Mass flow (unit-1) (Kg/s)	Average velocity (unit-4) (m/s)	Mass flow (unit-4) (Kg/s)
Plane-1	0.02511	1.185	0.568072	0.016902	0.232973	0.006932
Plane-2	0.02511	1.185	0.292622	0.008706	0.214130	0.006371
Plane-3	0.00686	1.185	0.214394	0.001743	0.175025	0.001423
Plane-4	0.02511	1.185	0.531576	0.015816	0.091812	0.002732
Plane-5	0.01464	1.185	0.331098	0.005744	0.171028	0.002967
Plane-6	0.00534	1.185	0.474072	0.002997	0.105644	0.000668

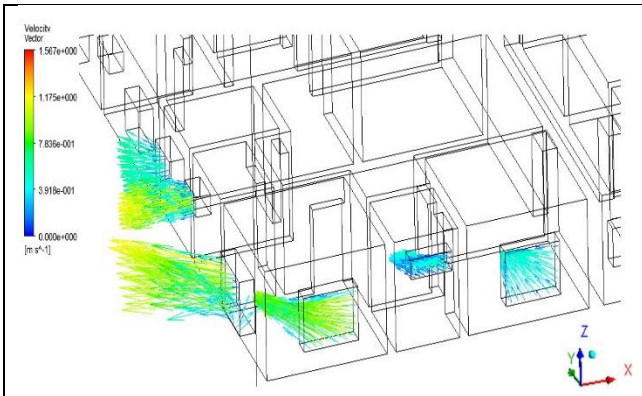

Fig.12: Velocity vectors through different windows of unit-1 of fifth floor with room partitions.

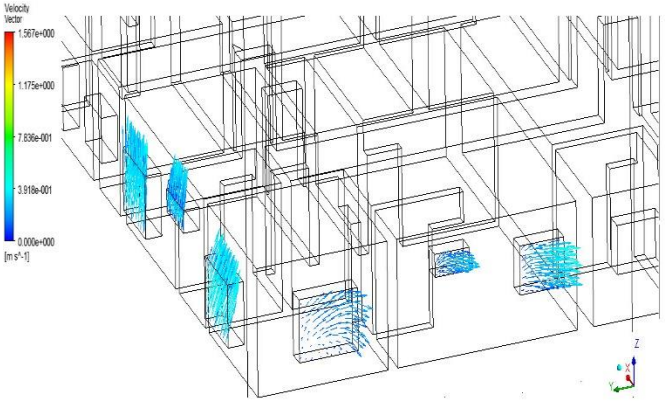

Fig.13: Velocity vectors through different windows of unit-4 of fifth floor with room partitions.

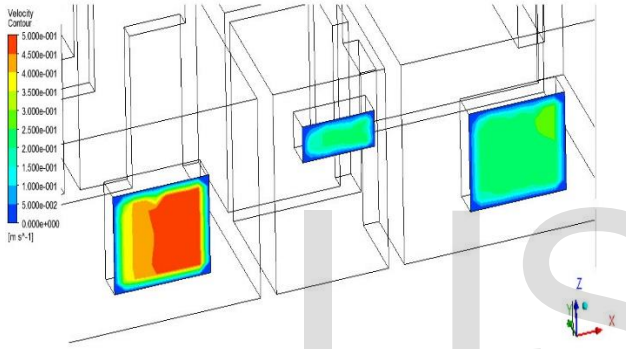

Fig.14(a): Velocity contours on south wall windows of unit-1 of fifth floor with room partitions.

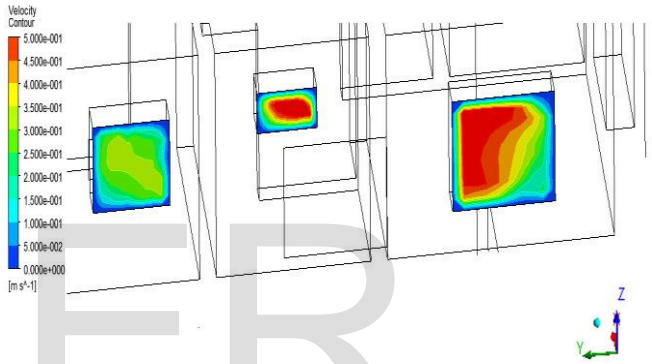

Fig.14(b): Velocity contours on west wall windows of unit-1 of fifth floor with room partitions.

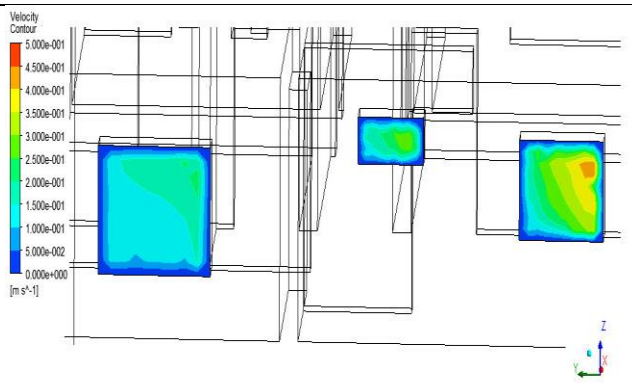

Fig.15(a): Velocity contours on west wall windows of unit-4 of fifth floor with room partitions.

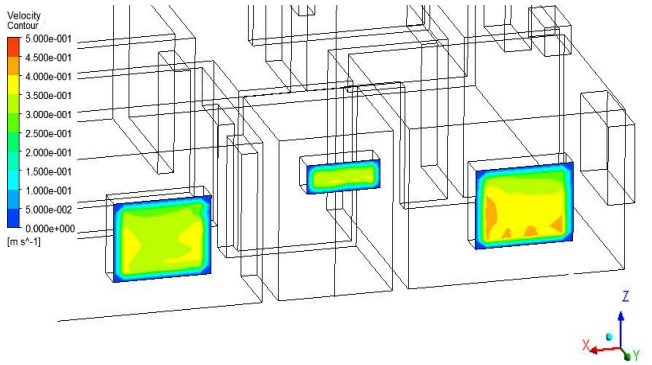

Fig.15(b): Velocity contours on north wall windows of unit-4 of fifth floor with room partitions.

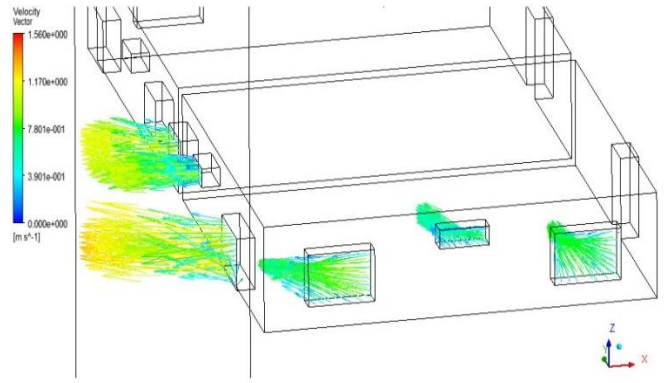

Fig.16: Velocity vectors through different windows of unit-1 of fifth floor without room partitions

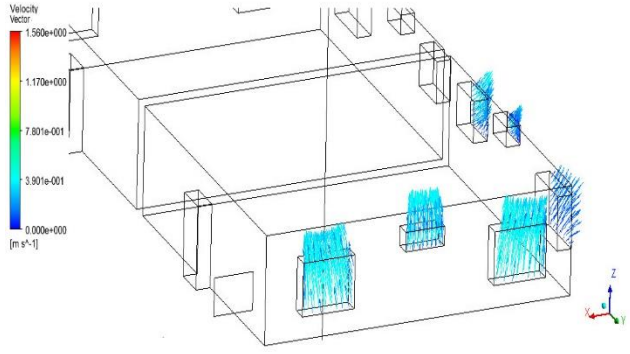

Fig.17: Velocity vectors through different windows of unit-4 of fifth floor without room partitions.

6.3 Comparison and flow analysis in unit-1 & unit-4 of second floor

Flow analysis in second floor (height = 3.3 m to 6.1 m) with and without the room partitions in unit-1 and unit-4 are reported in this section. Average mass flow in unit-1 and unit-4 using both cases, with and without room partitions in each unit is shown in Table-4. Similar mass flow as fifth floor is observed here. Fig. 18 to Fig. 22 show the velocity vectors and velocity contours through different windows of unit-1 and unit-4 for two different cases. South wall and north wall windows are working as inlet (Fig. 19 to Fig. 22). On the other hand, west wall windows are working as outlet for both the units (Fig. 19 to Fig. 22).

Mass flow is lower in case of with room partitions as expected than without partitions. In case of with partitions, inner walls retard the airflow. Mass flow may be lower for this reason. Mass flow is lower as fifth floor through the windows located in living room-1 and bath-1 (at south wall and north wall) for the position of openings in two adjacent walls. Mass flow may be increased if the windows and doors are located in two opposite walls.

Table 4
Average mass flow through different windows of unit-1 and unit-4 in second floor

Position	Area (m^2)	Density (Kg/m^3)	Mass flow in unit-1 (with-partition) (Kg/s)	Mass flow in unit-4 (with-partition) (Kg/s)	Mass flow in unit-1 (without-partition) (m/s)	Mass flow in unit-4 (without-partition) (Kg/s)
Plane-1	0.02511	1.185	0.01711	0.00717	0.56352	0.2116
Plane-2	0.02511	1.185	0.0167	0.0044	0.49016	0.1947
Plane-3	0.00686	1.185	0.00244	0.00098	0.37845	0.14474
Plane-4	0.02511	1.185	0.01416	0.00769	0.53109	0.32596
Plane-5	0.01464	1.185	0.00498	0.00045	0.56004	0.30396
Plane-6	0.00534	1.185	0.002	0.00088	0.42602	0.24132

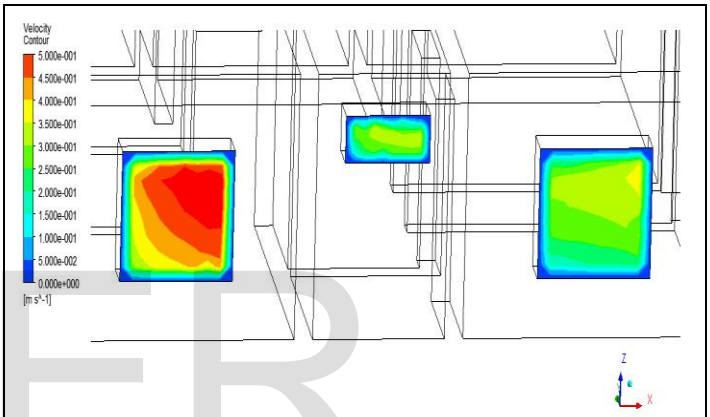

Fig.18(a): Velocity contours on south wall windows of unit-1 of second floor with room partitions.

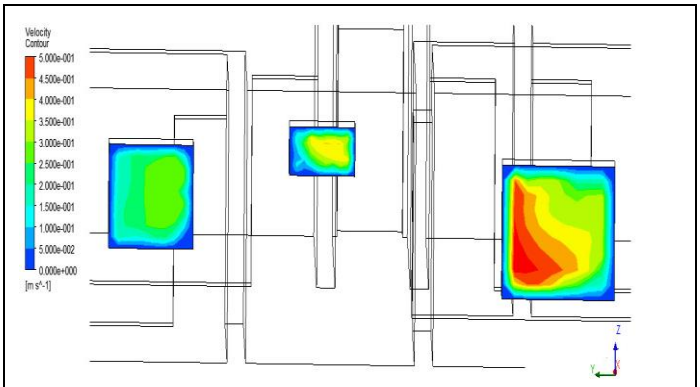

Fig.18(b): Velocity contours on west wall windows of unit-1 of second floor with room partitions.

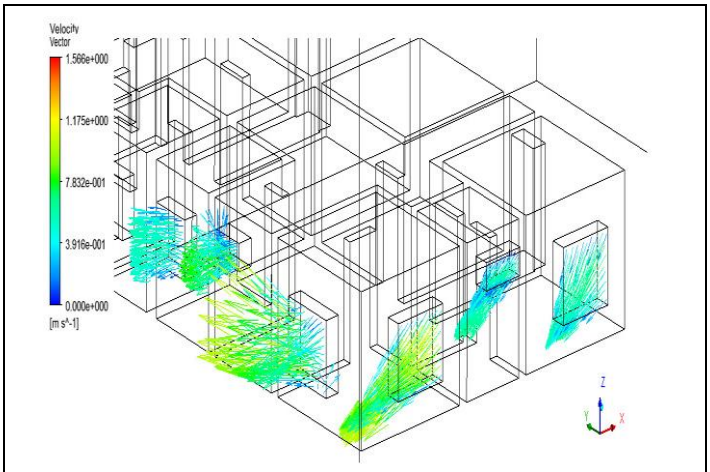

Fig.19: Velocity vectors through different windows of unit-1 of second floor with room partitions.

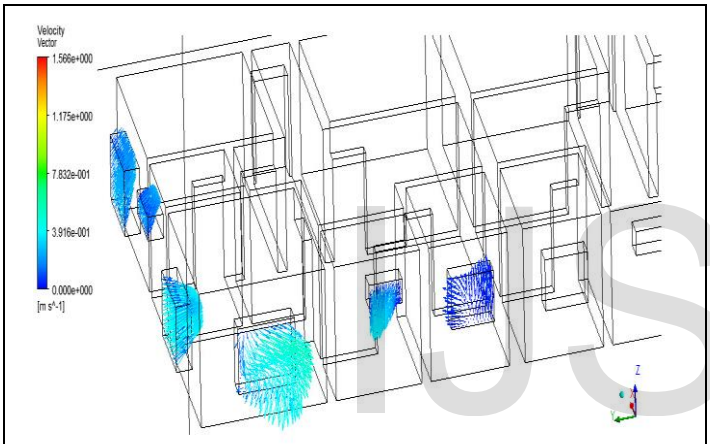

Fig.20: Velocity vectors through different windows of unit-4 of second floor with room partitions.

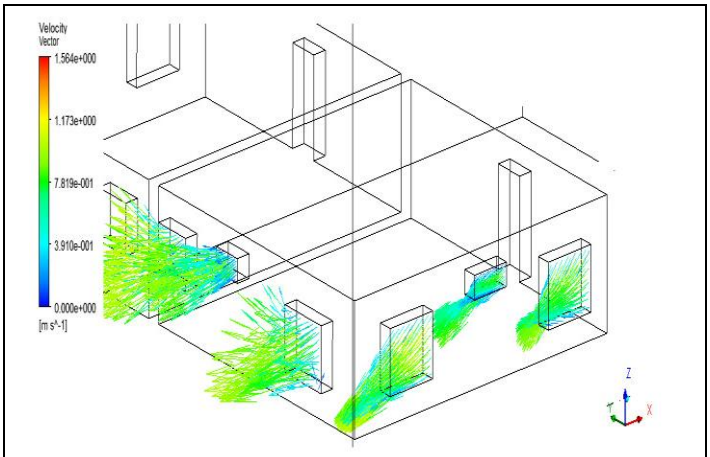

Fig.21: Velocity vectors through different windows of unit-1 of second floor without room partitions.

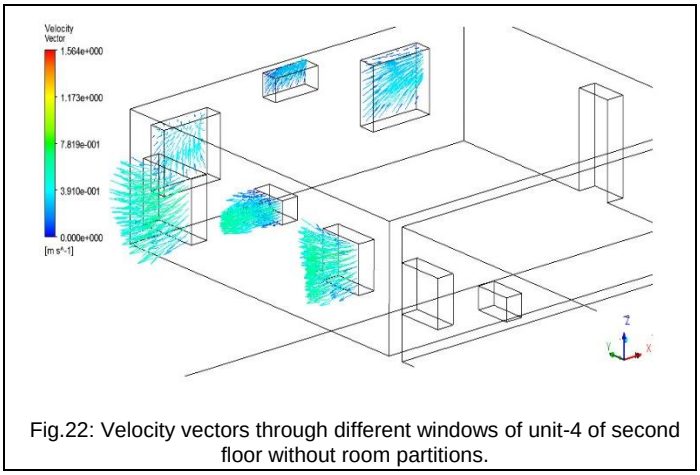

Fig.22: Velocity vectors through different windows of unit-4 of second floor without room partitions.

7 Ventilation rate

The required ventilation rate for each person (CEN-CR1752) for class C is 4.7 gm/s. From Table-5, it is observed that in this studied building ventilation rate is satisfactory for 6-8 persons in each unit. That means, Natural ventilation will be an important option to maintain the thermal comfort and quality of indoor air circulation of this building without using artificial mechanical systems. A lot of energy may be saved by using natural ventilation system in case of mechanical ventilation system. The solar chimney is a method to improve the natural ventilation of buildings by using convection of air heated passively by solar energy, a ventilation practice known from the roman times. The use of solar chimney for natural ventilation of buildings is a widely used architectural technique. To save the electricity consumption for this building, natural ventilation system may become a conducive instrument.

Table 5
Volume flow rate

Floor	Volume of Unit-1 (m^3)	Volume flow (gm/s)	Volume flow/hour (gm/h)	ACH
Eighth floor (without partition)	300.953	38.3	137880	2.59
Fifth floor (without partition)		32.03	115308	3.10
Second floor (without partition)		34.43	123948	2.87

8 Conclusion

An eight-storied building on a lot area of 7200 ft^2 (10 Katha) is chosen for numerical simulation enclosing 80% area (5760 ft^2) of total lot area to comply with the building code for Dhaka city. Each of the floors has four units of equal area (1400 ft^2). Simulations are done for eighth, fifth and second floors. Similarity in mass flow and heat transfer characteristics are observed for all three floors.

Similar mass flow distributions are observed for eighth, fifth and second floor. Velocity of the flow is found to be in decrease with the decrease of building height, which is also comparable with the inlet boundary condition. Velocity

vectors and velocity contours through different windows also gives similar results at each floor.

For unit-1, south wall windows work as inlet and west wall as outlet. But for unit-4 west wall windows works as outlet and north wall as inlet, thought north wall was considered as outlet during simulation. It may be because of the density difference of air in and outside the building.

Ventilation rate is also found to be satisfactory in this building without any mechanical support. So, by following the building code properly satisfactory ventilation rate can be assured only by natural ventilation system or a moderate use of mechanical support at lower floors.

Acknowledgement:

1. Project Under special allocation for Science and Technology 2014-2015, Ministry of Science and Technology, Bangladesh.
2. Computational facilities available in the Department of Applied Mathematics, University of Dhaka, Dhaka 1000, Bangladesh.

References:

[1] A. S. M. Mahbubun Nabi, Md. Kamruzzaman, Wahida Khalil, Fahmida Khandokar, June 2004, Apartment Housing in High Class Residential Areas of Dhaka City: A Case Study of Dhanmondi, Gulshan and Baridhara, Jahangir nagar Planning Review, ISSN 1728-4198 Vol. 2(33-42).

[2] Bangladesh National Building Code-2012.

[3] An-Shik Yang, Chih-Yung Wen, Yu-Chou Wu, Yu-Hsuan Juan, and Ying-Ming Su,WCE 2013 (July 3-5), Wind Field Analysis for a High-rise Residential Building Layout in Danhai, Taiwan, , Proceedings of the World Congress on Engineering 2013 Vol II, London, U.K.

[4] ANSYS 12.0, Ansys Inc., User manual.

[5] G. Evola, V. Popov,2006, Computational analysis of wind driven natural ventilation in buildings, Energy and Buildings 38 (491–501).

[6] Jantunen, M., 2000, 'When and where are people exposed to pollutants,' Human Responses and Building Investigations Proceedings, Vol. 1. (15–22).

[7] Kuo, N.W., Chiang, H.C., Chiang, C.M., 2008, 'Development and application of an integrated indoor air quality audit to an international hotel building in Taiwan,' Environmental Monitoring and Assessment, Vol. 147, No. 1, (139-147).

[8] Manfred J. Zapka, Tuan Tran, A. James Maskrey, Stephen Meder, 2014, Computational Fluid Dynamics (CFD) Applications at the School of Architecture, Project Phase 1 – 7.B, Develop Skill Set for Internal CFD Analysis and Verification at the Building, Hawaii Natural Energy Institute (HNEI), University of Hawaii.

[9] M. F. Mohamed, S. King, M. Behnia, D. Prasad, J. Ling,2010, Wind-driven natural ventilation study for multi-storey residential building using CFD, 44th Annual Conference of the Architectural Science Association, ANZAScA Unitec Institute of Technology.

[10] P. Karava, T. Stathopoulos, A.K. Athienitis, 2011, Airflow assessment in cross-ventilated buildings with operable façade elements, Building and Environment 46 (266-279).

[11] Qingyan Chen, 2008, Ventilation performance prediction for buildings: A method overview and recent applications, Building and Environment, 44(4), 848-858.

[12] R. Ramponi, B. Blocken, 2012, CFD simulation of cross-ventilation for a generic isolated building: Impact of computational parameters, Building and Environment 53(34-48).

[13] Saiful Islam, 10-12 September, 2013, Impacts of 'Maximum Allowable Building Footprint' on Natural Ventilation in Apartment Building, PLEA 2013 - 29th Conference, Sustainable Architecture for a Renewable Future, Munich, Germany.

[14] Saiful Islam, 2012, A study on zoning regulations' Impact on Ventilation Rate' in non-conditioned apartment buildings in Dhaka city, proceedings of the solar conference, World renewable energy forum, American solar energy society, vol. 5, (3584-3591).

[15] Saiful Islam, CAA Dhaka-2013, An Extended Study on Building Regulations 'Impact on Natural Ventilation in Apartment Buildings in Dhaka City, 20th general Assembly and Conference.

[16] Saiful Islam, 10-12 September 2013, Impacts of 'Maximum Allowable Building Footprint' on Natural Ventilation in Apartment Building, PLEA 2013 - 29th Conference, Sustainable Architecture for a Renewable Future, Munich, Germany.

[17] Ventilation for Acceptable Indoor Air Quality, ANSI/ASHRAE Standard 62.1-2004.

[18] W. Ding, Y. Hasemi, T. Yamada, Apr. 2005, "Natural ventilation performance of a double-skin façade with a solar chimney," Energy Build., vol. 37, no. 4, (411–418).

[19] W. Oesterle, E. Lieb, R-D. Lutz, M. Heusler, 2001, "Double skin facades – Integrated planning," Prestel Verlag Munich.